PAPER

Open crack depth sizing by laser stimulated infrared lock-in thermography

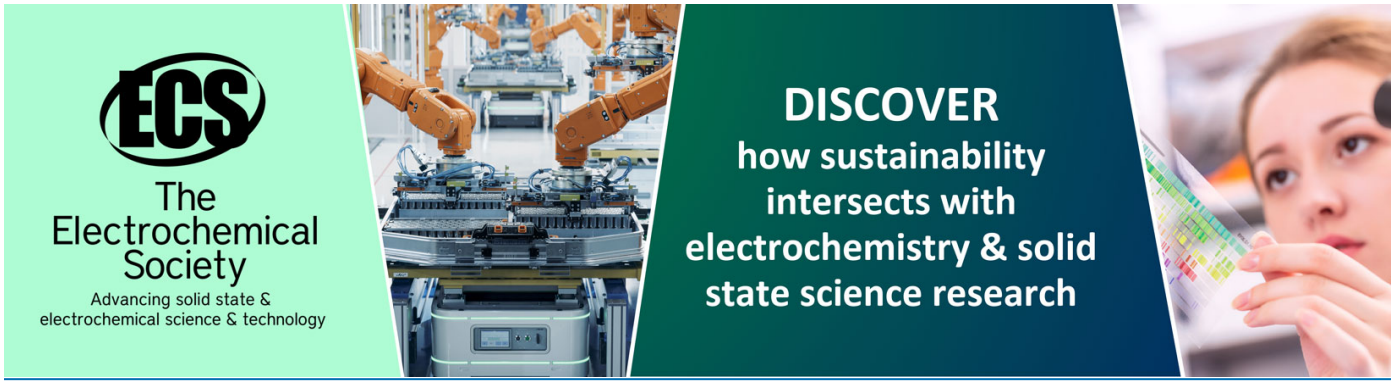

IOP Publishing Journal of Physics D: Applied Physics
J. Phys. D: Appl. Phys. **47** (2014) 465501 (6pp) doi:10.1088/0022-3727/47/46/465501

Open crack depth sizing by laser stimulated infrared lock-in thermography

Y Fedala[1,2], M Streza[3], J-P Roger[2,4], G Tessier[2,4,5] and C Boué[6,7,8]

[1] Département de Biologie, Ecole Normale Supérieure, 46 rue d'Ulm, 75005 Paris, France
[2] CNRS, UMR 7587, Institut Langevin, 1 rue Jussieu, F-75005, Paris, France
[3] NIR&DIMT, 65–103 Donath Street, 400293 Cluj-Napoca, Romania
[4] ESPCI ParisTech, PSL Research University, Institut Langevin, 1 rue Jussieu, F-75005, Paris, France
[5] Wavefront Engineering Microscopy Group, Neurophotonics Laboratory, CNRS UMR 8250, University Paris Descartes, Sorbonne Paris Cité, 75006 Paris, France
[6] LPEM, PSL Research University, ESPCI-ParisTech, 10 rue Vauquelin, F-75231 Paris Cedex 5, France
[7] Sorbonne Universités, UPMC Univ Paris 06, F-75005 Paris, France
[8] CNRS, UMR 8213, F-75005 Paris, France

E-mail: christine.boue@espci.fr

Received 2 June 2014, revised 1 September 2014
Accepted for publication 15 September 2014
Published 29 October 2014

Abstract
Recent advances in infrared imaging have made active thermography an interesting non destructive technique for sub-surface defect detection. Here, we present a method for the estimation of the depth of open surface defects by infrared lock-in thermography, based on the relation between the crack depth and the Laplacian of the surface temperature distribution induced by a local heating using a laser. A comparison to numerical finite element modelling for different depths allows an accurate determination of fatigue crack depth in Inconel alloy test blocks.

Keywords: crack depth estimation, infrared lock-in thermography, finite element methods, image processing

(Some figures may appear in colour only in the online journal)

1. Introduction

Systems that are submitted to mechanical stress usually develop defects which influence their stiffness and lead to failure. More than localization, depth is an essential information to appreciate the possible dangerousness of a crack. Testing for these defects in 3D is therefore of particular importance.

Liquid penetrant has been the most common method to detect cracks [1], but this technique cannot give much quantitative information on the depth of the defect. Ultrasounds [2] or Eddy Currents [3], can provide some quantitative estimation, but they require a contact with the sample, which makes them unsuitable for several inaccessible structures or samples with irregular geometries.

In the most common types of non-destructive testing thermography, a broad area of the object is heated by high power flash lamps. The thermal energy deposited on the surface diffuses across the surface and into the bulk. The presence of a crack changes the heat diffusion process and thus the thermal footprint. Infrared thermography has been successfully used in detecting defects such as impact damage [4, 5], delaminations [5], and material loss defects [6]. However, cracks oriented perpendicular to a surface cannot be detected with 1D surface heating. Lateral thermal flows are indeed essential in order to detect vertical cracks. They can be generated with for instance a localised heating, either on the surface of the tested material using optical sources, or in the bulk using ultrasounds or eddy currents [7, 9].

Most methods take advantage of the wave-like properties of the heating induced by space or time modulated excitations, in order to control localization or to enhance signal to noise ratio using lock-in detection [10]. Among these methods, lock-in thermography is increasingly exploited for the quantitative evaluation of defects [11–13]. The amplitude and phase infrared images obtained by the diffusion of lateral thermal

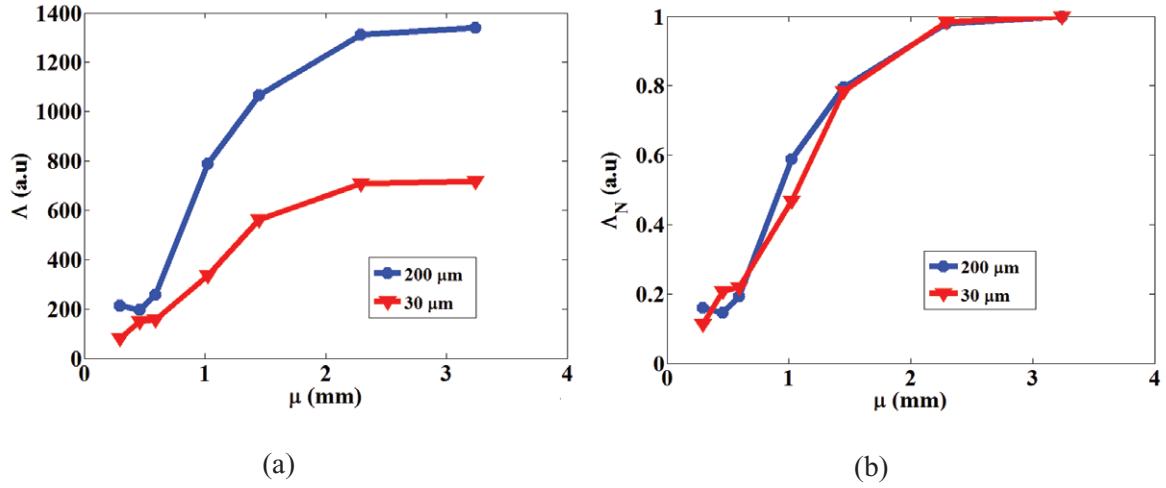

Figure 1. (*a*) $\Lambda(\mu)$ for two widths: $l = 30\mu$m and $l = 200\mu$m. (*b*) $\Lambda_N(\mu)$ for two widths: $l = 30\mu$m and $l = 200\mu$m. The modulation frequency f is chosen between 0.1 and 10 Hz. Finite elements simulation performed with the parameters: $\alpha = 3.3\,\text{m}^2/\text{s}$, $h = 2$ mm, $r = 0.5$ mm and $d = 1.5$ mm. The crack length L is equal to 9 mm.

flows provide information concerning hidden defects with a good contrast for vertical cracks [9]. The flying spot technique [14–16] which uses a line-shaped laser beam that is scanned over the investigated surface needs calibration curves to have an evaluation of the crack depth. Other methods exploit the asymmetry of the thermal footprint of a laser spot in the vicinity of a crack [17–20] or combined lock-in infrared thermography and ultrasounds (lock-in vibrothermography [21]).

The objective of this work is to use a lock-in thermography procedure for depth evaluation of surface-breaking cracks in metals without surface preparation. We report the implementation of the approach described in [22, 23] to evaluate linear open surface cracks by the means of lock-in thermography, and provide crack depth determination, taking advantage of the modulation frequency and thermal diffusion length to probe different regions of the sample. This approach exploits the evolution of the second order derivative of the amplitude image as a function of the thermal diffusion length. First, a specific data analysis to extract quantitatively the value of the crack depth independently of its width is presented. Then, an abacus obtained by numerical simulation is used to deduce the crack depth for a material with a known diffusivity.

2. Principle of the method: probing cracks by frequency analysis

In this work, a modulated laser spot excitation heats the sample surface. Using a lock-in thermography detection, the unwanted dc component which depends on the emissivity of the materials and on the ambient temperature is filtered out from the raw images of the IR camera. The modulated component of the IR emission induced at the surface of the inspected sample by the thermal diffusion is then extracted with an excellent contrast. In the presence of cracks, which act as thermal barriers, thermal diffusion is disrupted. The spatial second derivative of the amplitude image highlights the thermal wave disturbance caused by these cracks.

In this work, the thermal diffusion length, which can be adjusted by changing the modulation frequency, is used as a 3D probe of the crack depth. The crack signature is analyzed via the changes of the spatial second order derivative of the amplitude image versus the thermal diffusion length. The evolution of this function allows the depth of a crack perpendicular to the surface to be deduced.

In the methods and experiments described here, a laser beam is focused to a circular and uniform spot of radius r to heat up the sample at a distance d from the nearest edge of a crack in a metal surface. This heating amplitude is square-wave modulated.

A lock-in processing of the signal allows a retrieval of both amplitude and phase of the sinusoidal infrared radiation component at the fundamental frequency f. The thermal diffusion length is: $\mu = \sqrt{\alpha / \pi f}$, where α is the thermal diffusivity of the specimen. Notice that diffusivity can be directly extracted from measurements [24].

Since the crack behaves as a thermal barrier, the crack should be located inside the heat diffusion region, within a distance from the source of the order of the thermal diffusion length in order to optimally characterize the defect of the investigated structure. By varying the modulation frequency f, the thermal diffusion length μ can be changed. For μ smaller than the distance d between the heat source and the crack edge, the modulated part of the heat flux that reaches the crack before vanishing is very small. In the special case where the diffusion length is of the order of the distance to the crack, the heat flux reaches the edge of the crack on the surface and then is blocked. For longer diffusion lengths, the heat flux diffuses deeper into the volume along the crack and may bypass the defect.

Thus, using a modulated excitation associated to lock-in thermography, the excitation frequency offers a way to change the size of the modulated heat diffusion region. The second order spatial derivative (Laplacian) of the amplitude image is then calculated in order to emphasize the perturbative effects of cracks on thermal *waves* [20]. In previous work [21], a function $\Lambda(\mu)$, which is the absolute value of the Laplacian

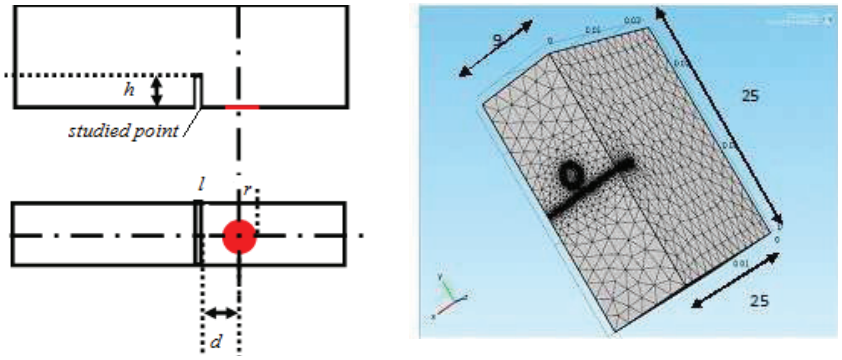

(a) (b)

Figure 2. (*a*) Top and front views of the specimen heated by a circular beam of radius *r* at a distance *d* from the nearest edge of the defect. The depth of the crack is given by *h* and the width by *l*. (*b*) Typical mesh for FEM simulations of the specimen of thermal diffusivity α heated by a circular laser beam. The smallest mesh element size was chosen three times smaller than the width of the crack itself. The heat source is a disc of radius *r* at a distance *d* from the nearest edge of the defect.

of the amplitude image obtained at frequency *f* was proposed. Simulation results show that $\Lambda(\mu)$ obtained from the crack signature depends on the geometry (depth and width) of the crack [21].

When both depth and width are unknown, the depth evaluation is therefore difficult. In this work we propose a new function which mainly depends on the depth of the crack.

3. Normalized Λ function

In the following simulation results, the evolution of Λ as a function of μ is extracted from a point located on the edge of the crack which faces the heating zone center.

The Λfunction increases with the crack depth or width, and reaches a horizontal asymptote when the thermal diffusion region is larger than the crack, as can be seen in figure 1(*a*) in the case of cracks having the same depth *h* but different widths *l*. The saturation level for the width $l = 30\,\mu$m is lower than for the width $l = 200\,\mu$m.

To overcome this problem, we consider $\Lambda_N(\mu)$, the values of $\Lambda(\mu)$ normalized by its maximum value, provided that the chosen range of thermal diffusion lengths is sufficient to reach the $\Lambda(\mu)$ plateau. As can be seen in figure 1(*b*), the evolution of Λ_N as a function of the diffusion length μ is then independent of the crack width.

4. Simulation results: defect depth abacus

The effect of a modulated localized heat flux on a cracked surface is modeled by Finite Element Method (FEM) using COMSOL and a heat transfer module. The developed model (figure 2(*a*)) considers the same geometrical parameters as the sample used in the experimental part. A mesh example is shown in figure 2(*b*).

Dimensions of the block: 25 × 25 × 9 mm^3. $\alpha = 3.310^{-6}$ m^2 s^{-1}, *r*=0.5 mm, $d = 1.3$ mm, $h = 2$ mm and $l = 30\,\mu$m.

3D simulations have been performed for an excitation frequency ranging from 0.06 to 4.2 Hz, for different crack depths *h*, keeping constant the absorbed laser power and the distance

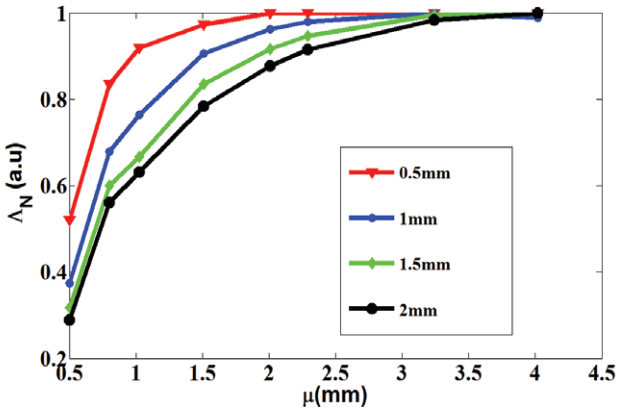

Figure 3. Evolution of Λ_N as a function of μ calculated by FEM for different values of *h* for $d = 1.3$ mm. The modulated frequency *f* is chosen between 0.06 and 4.2 Hz.

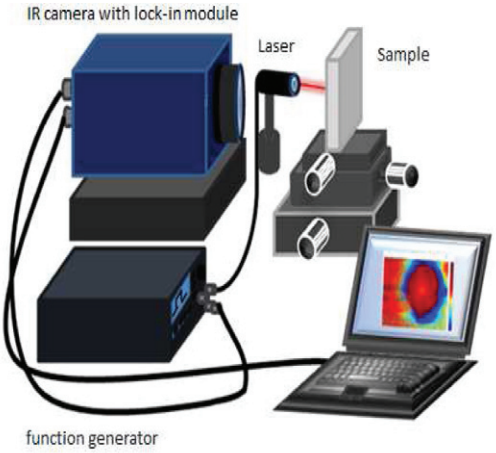

Figure 4. Experimental set-up.

d between the center of the laser spot and the edge of crack. The evolution of $\Lambda_N(\mu)$ as a function of the thermal diffusion length is shown in figure 3 for different values of *h* chosen between 0.5 and 2 mm.

One can observe that the $\Lambda_N(\mu)$ curves depend on the crack depth. The evaluation of the position of the shoulder in the

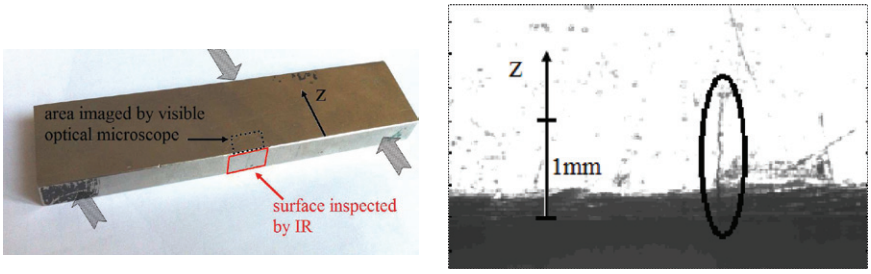

(a) (b)

Figure 5. (*a*) Photography of sample B. The shaded arrows indicate the pressure points used to create the crack. (*b*) Visible optical microscopy allows to measure the propagation distance of the fatigue crack (in the ellipse) on the lateral sides.

Table 1. Sample sizes measured by visible optical microscopy.

	Depth (mm) on the two lateral sides of the sample	averaged depth (mm) deduced from the values of the first column	crack width (μm)
Sample A	1.0 ± 0.1 and 2.1 ± 0.1	1.5	40 ± 0.5
Sample B	1.1 ± 0.1 and 3.1 ± 0.1	2.1	35 ± 0.5
Sample C	1.7 ± 0.1 and 2.4 ± 0.1	2	65 ± 0.5

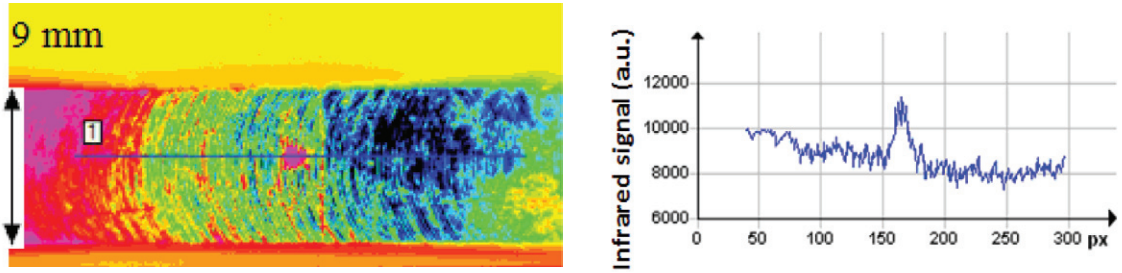

(a) (b)

Figure 6. (*a*) IR DC image in the presence of an excitation at frequency $f = 0.2$ Hz (sample B); (*b*) amplitude profile along marker 1 (1 pixel, px, corresponds to 50 μm) in (*a*). IR results obtained with Inconel samples heated by a modulated 2 W laser are displayed in figures 6 and 7.

evolution of Λ_N with μ is a good indicator of the crack depth. These curves obtained by simulation can therefore be used as an abacus to determine crack depths of studied samples.

In conclusion, the analysis of the $\Lambda_N(\mu)$ function allows the depth of the defect to be estimated, independently to its width (as shown in section 3 [25]).

5. Experimental results for the depth evaluation

5.1. Experimental set-up

The experimental set-up shown in figure 4 includes a heat source (a diode-pumped Ytterbium laser with 830 nm wavelength and tuneable power), a function generator, and an infrared camera (Jade III, CEDIP, FLIR), which has an array of 240 × 320 of InSb detectors sensitive in the 3–5 μm wavelength range. The acquisition frequency of the camera is 100 Hz.

The laser light outgoing from the multimode fiber is focused onto the surface in an approximately uniform and circular spot of 1 mm diameter. The intensity-modulated optical stimulation has been targeted in the vicinity of the crack, at a distance d. The signals delivered by the infrared camera and the reference frequency f are sent to a lock-in detection module (FLIR R9902), which provides the continuous component image ($f = 0$) as well as the amplitude and phase images of the f-component to a computer. The acquisition duration depends on the solicitation frequency f: the lower the frequency, the longer the duration (around 1 min at f =0.1 Hz).

5.2. Experimental determination of a crack depth

Three open vertical fatigue cracks (Sample A, Sample B and Sample C) of 35–65 μm width were obtained by exerting pressure on 2 extremities of the samples, while keeping 1 point fixed at the center of the opposite facet (see shaded arrows in figure 5). These model samples are made of highly reflecting 130 × 27 × 9 mm^3 Inconel metallic plates (figure 5(*a*)). Using optical microscopy, it was possible to estimate the depth of the defect on the lateral sides of the sample (see table 1) since the crack is open all along the sample and is visible (figure 5(*b*)).

Because these specimens are highly reflective, the reflected and emitted infrared radiation varies sharply in the presence of surface roughness, and consequently the DC image is strongly disturbed (figure 6). A heated area due to the laser absorption at the sample surface is guessed in the center of the figure 6(*a*)

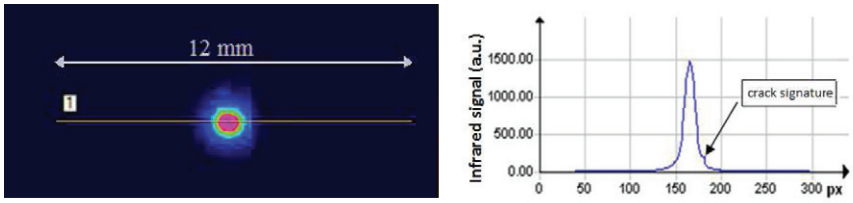

(a) (b)

Figure 7. IR amplitude image at the excitation frequency (f=0.2 Hz) obtained by lock-in detection (sample B). (b) Amplitude profile along marker 1 (1 pixel, px, corresponds to 50 μm) in (a).

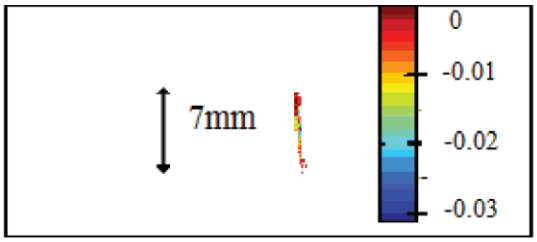

Figure 8. Λimage obtained for f=0.2 Hz (sample B).

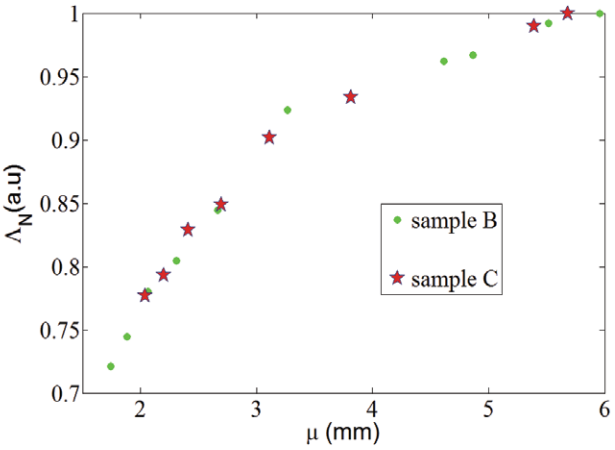

Figure 9. Experimental Λ_N values obtained with B and C samples d = 1.1 mm. The modulated frequency f is chosen between 0.03 and 0.3 Hz.

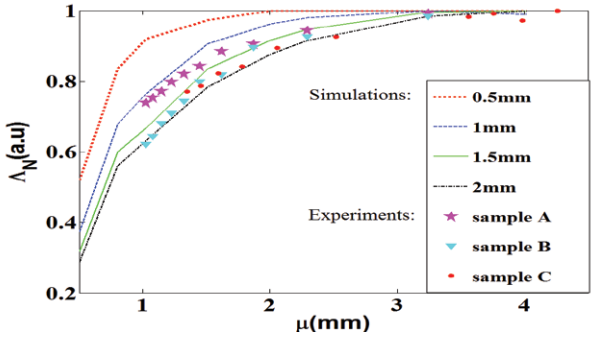

Figure 10. Experimental Λ_N values obtained on Inconel alloy samples superimposed on the abacus of the simulated evolutions of Λ_N obtained by FEM for different values of h in the 0.5–2 mm range, and for d=1.3 mm. The modulation frequency f for the experiments is chosen between 0.06 and 1 Hz.

Table 2. Thermography results.

	Crack depth h (mm) evaluated by thermography
Sample A	1.2 ± 0.2
Sample B	1.8 ± 0.3
Sample C	1.8 ± 0.3

but no crack footprint appears in the DC image in figure 6(b) which is the cross section along the line shown in figure 6(a). Using the lock-in detection system, however, the image of the magnitude at the excitation frequency f has been obtained (figure 7). We can observe on the surface of the sample that the heat diffusion around the heated area is interrupted on the right of the heated area (figure 7(a)) which reveals a crack. It is also clearly visible in the cross section (figure 7(b)). The second order spatial derivative of figure 7 is then calculated to obtain the Λimage (figure 8): a crack appears clearly. Applying the analysis procedure previously described in section 3, the evolution of $\Lambda_N(\mu)$ can be calculated.

First, we verify experimentally that, as shown above using FEM calculations, the sample crack width has no influence on the evolution of Λ_N. Figure 9, which represents the measured $\Lambda_N(\mu)$ curves obtained for samples B and C characterized by the same averaged depth but not the same crack width, shows that the $\Lambda_N(\mu)$ curves are indeed independent on sample width.

Figure 10 presents the measured $\Lambda_N(\mu)$ values obtained for samples A and B. These are superimposed with the simulation results for different excitation frequencies (i.e. different diffusion lengths μ) for different depths (as shown in figure 3).

One can see in figure 9 that the behavior for experimental $\Lambda_N(\mu)$ values is similar to the simulation curves. Therefore, the simulation results can be used as an abacus allowing the quantitative determination of the depth of the cracks. Results on sample A are contained between the 1 and 1.5 mm simulation curves and, on sample B and C, between 1.5 and 2 mm. Consequently, the depth of the cracks is evaluated by averaging these values to 1.2 ± 0.2 mm for sample A and to 1.8 ± 0.3 mm for samples B and C respectively. This is in good agreement with the averaged depths deduced from optical microscopy measurements (see table 1), showing that a confrontation of the experimental results with the abacus obtained by FEM simulations allows to find a good evaluation of the crack depth of samples (see table 2).

These results will of course benefit from thorough testing and error evaluation on various sample sizes and composition,

but they offer a good experimental indication that, in samples with known thermal properties, Finite Element Methods can be used to produce abacuses allowing the quantitative determination of crack depths by comparison with experimental measurements.

6. Conclusion

A lock-in thermography technique using a frequency analysis combined to efficient image processing is presented. We propose the use of a function $\Lambda_N(\mu)$ (normalized Laplacian of the amplitude of the modulated surface temperature) to estimate the depth of surface open cracks without any assumption regarding the width of the considered crack. The proposed technique is experimentally validated with 3 different Inconel test blocks for the evaluation of surface-emerging fatigue cracks. The experimental results compared to numerical simulations show that the depth of the defects can be well estimated by the presented method using a calibration abacus obtained by FEM simulation.

It is shown that the developed method is well adapted to measure crack depths in the 0.5–3 mm range. It is suitable for local crack depth evaluation. Indeed, for a well known sample (known diffusivity and calculated abacus) the measurement duration is mainly due to the time of lock-in acquisition which depends on the number of chosen heating frequencies and on the value of the lower frequency. We can consider that the time evaluation of one crack depth is typically 10 min. In addition, for some samples with crack width larger than the camera pixel resolution, the contribution of crack emissivity should be taken into account.

Acknowledgments

This work was supported by the 'Pôle ASTech' and the 'Pôle Nucléaire de Bourgogne', and has been funded by the Ville de Paris, France.

The authors would like to thank Areva Intercontrole for providing Inconel 690 samples with various calibrated fatigue cracks, and Stephane Holé for fruitful proofreading of the present manuscript.

References

[1] Cartz L 1995 *Nondestructive Testing* (Materials Park, OH: ASM International)
[2] Achenbach J D 1992 Mathematical modeling for quantitative ultrasonics *Nondestr. Test. Eval.* **8** (9) 363–77
[3] Auld B A and Moulder J C 1999 Review of advances in quantitative eddy current nondestructive evaluation *J. Nondest. Eval.* **18** 441–8
[4] Vavilov V P, Almond D P, Busse G, Grinzato E, Krapez J-C, Maldague X, Marinetti S, Peng W, Shirayev V and Wu D 1998 Infrared thermographic detection and characterization of impact damage in carbon fibre composites: results of the round robin test *Proc. QIRT 98* (*Paris*) ed D Balageas *et al* (Paris: EETI editions) pp 43–52
[5] Ibarra-Castanedo C, Avdelidis N P, Grinzato E G, Bison P G, Marinetti S, Plescanu C, Bendada A and Maldague X 2011 Delamination detection and impact damage assessment of GLARE by active thermography *Int. J. Mater. Prod. Technol.* **41** 5–16
[6] Marinetti S and Vavilov V 2010 IR thermographic detection and characterization of hidden corrosion in metals: general analysis *Corros. Sci.* **52** 865–72
[7] Dillenz A, Zweschper T, Riegert G and Busse G 2003 Progress in phase angle thermography *Rev. Sci. Instrum.* **74** 417–19
[8] Weekes B, Almond D P, Cawley P and Barden T 2012 Eddy-current induced thermography—probability of detection study of small fatigue cracks in steel, titanium and nickel-based superalloy *NDT E Int.* **49** 47–56
[9] Lugin S 2013 Detection of hidden defects by lateral thermal flows *NDT E Int.* **56** 48–55
[10] Gleiter A, Spießberger C and Busse G 2010 Lock-in thermography with optical or ultrasound excitation *J. Mech. Eng.* **56** 619–24
[11] Peng D and Jones R 2013 Lock-in thermographic inspection of squats on rail steel head *Infrared Phys. Tech.* **57** 89–95
[12] Wallbrink C, Wade S A and Jones R 2007 The effect of size on the quantitative estimation of defect depth in steel structures using lock-in thermography *J. Appl. Phys.* **101** 104907
[13] Choi M, Kang K, Park J, Kim W and Kim K 2008 Quantitative determination of a subsurface defect of reference specimen by lock-in infrared thermography *NDT E Int.* **41** 119–24
[14] Gruss C, Lepoutre F and Balageas D 1993 Nondestructive evaluation using a flying-spot camera *Proc. of 8th Int. THERMO Conf.* (*Budapest*)
[15] Krapez J-C, Legrandjacques L, Lepoutre F and Balageas D 1998 optimization of the photothermal camera of crack detection *QIRT 1998 Archives: Documents and Sessions Presented during the 4th Conf. on QIRT* (*Lodz, Poland*)
[16] Netzelmann U 2014 Flying-spot lock-in thermography and its application to thickness measurement and crack detection *QIRT2014, 12th Int. Conf. on Quantitative Infrared Thermography (Bordeaux, France)*
[17] Schlichting J, Ziegler M, Dey A, Maierhofera Ch and Kreutzbruck M 2011 Efficient data evaluation for thermographic crack detection *Quant. Infrared Thermolgr. J.* **8** 119–23
[18] Schlichting J, Maierhofer Ch and Kreutzbruck M 2012 Crack sizing by laser excited thermography *NDT E Int.* **45** 133–40
[19] Li T, Almond D P and Rees S 2011 Crack imaging by scanning pulsed laser spot thermography *NDT E Int.* **44** 216–25
[20] Li T, Almond D P and Rees D A S 2011 Crack imaging by scanning laser line thermography and laser spot thermography *Meas. Sci. Tech.* **22** 035701
[21] Mendioroz A, Castelo A, Celorrio R and Salazar A 2013 Characterization of vertical buried defects using lock-in vibrothermograhy: I. Direct problem *Meas. Sci. Tech.* **24** 065601
[22] Fedala Y, Streza M, Sepulveda F, Roger J-P, Tessier G and Boué C 2014 Infrared lock-in thermography crack localization on metallic surfaces for industrial diagnosis *J. Nondestruct. Eval.* **33** 335–41
[23] Streza M, Fedala Y, Roger J-P, Tessier G and Boué C 2013 Heat transfer modeling for surface crack depth evaluation *Meas. Sci. Technol.* **24** 045602
[24] Boué C and Holé S 2012 Infrared thermography protocol for simple measurements of thermal diffusivity and conductivity *Infrared Phys. Tech.* **55** 376–79
[25] « Procédé d'évaluation de la profondeur d'une fissure » *French Patent* Application n° 12 58940, PCT/FR2013/052185, CNRS—UPMC. Inventors: BOUE Christine—TESSIER Gilles—ROGER Jean-Paul—STREZA Mihaela